American Mineralogist, Volume 69, pages 472–480, 1984

Donpeacorite, $(Mn,Mg)MgSi_2O_6$, a new orthopyroxene and its proposed phase relations in the system $MnSiO_3$–$MgSiO_3$–$FeSiO_3$[1]

ERICH U. PETERSEN,[2] LAWRENCE M. ANOVITZ, AND ERIC J. ESSENE

Department of Geological Sciences
University of Michigan, Ann Arbor, Michigan 48109

Abstract

A Mn-rich orthopyroxene $Mg_{1.41}Mn_{0.56}Ca_{0.03}Si_2O_6$, occurs in a manganiferous pod in the marble units near Balmat, N. Y. The pyroxene coexists with triodite, tourmaline, ferrian braunite, manganoan dolomite, and hedyphane. Refinement of the crystal structure of the pyroxene (space group *Pbca*) shows that as expected virtually all of the Mn is located in the M2 site and the general formula is therefore $(Mn,Mg)MgSi_2O_6$. Because Mn is completely ordered into the M2 site and comprises over 50 percent of that site, the mineral is a new orthopyroxene. It has been named donpeacorite after Donald R. Peacor in recognition of his work on pyroxenes and manganese minerals. The unit cell parameters are a = 18.384(11), b = 8.878(7), c = 5.226(3), Z = 8, D (meas.) = 3.36(1). Donpeacorite is biaxial negative with $2V_x = 88°$, $Z \| c$, α = 1.677(2), β = 1.684(2), γ = 1.692(2). It is yellow-orange with a vitreous luster and has an approximate hardness of 5–6 with perfect (110) cleavages.

The occurrence of donpeacorite and published data for metamorphic pyroxenes and pyroxenoids permit modeling of a phase diagram for the system $MnSiO_3$–$MgSiO_3$–$FeSiO_3$. The diagram is dominated by extensive fields for solid solutions of orthopyroxene and of pyroxmangite, with a small field inferred for kanoite ($MnMgSi_2O_6$, *C2/c* clinopyroxene) and a three-phase field for ferroan kanoite, manganoan hypersthene, and magnesian pyroxmangite.

Introduction

Several Mn-bearing minerals have been described from the manganoan pods in the Balmat, New York area including tirodite (Ross et al., 1969), magnesian rhodonite (Peacor et al., 1978), calcian kanoite, braunite, and hollandite (Brown et al., 1979; Gordon et al., 1981). Typically these minerals at Balmat form pink- to buff-colored rocks which contrast strikingly with the enclosing rocks. They may fluoresce a deep red when exposed to ultraviolet light and thus have received attention well beyond their abundance. Spectacular yellow-orange rocks containing an unusual Mn-rich pyroxene were collected on the 2500 level of the Balmat No. 4 Mine and provided for our study by John T. Johnson and William deLorraine of the St. Joe Zinc Company, Balmat, N. Y. X-ray diffraction studies and a structure refinement of the pyroxene indicate that it is orthorhombic and completely ordered with over half of the M2 site occupied by Mn. This orthopyroxene therefore qualifies as a new mineral and has been named donpeacorite after Dr. Donald R. Peacor of the University of Michigan Department of Geological Sciences, in recognition of his work with manganese minerals, as well as with pyroxenes and pyroxenoids. The name donpeacorite applies to the ordered orthopyroxene of endmember composition $MnMgSi_2O_6$. Thus the mineral described herein is $Dp_{56}En_{44}$. Both the mineral and the name donpeacorite has been approved by the I.M.A. Commission on New Minerals and Mineral Names (A. Kato, written connunication, 1982). Type material is preserved at the Smithsonian Institution, Washington D. C.

Mn-rich pyroxenes and pyroxenoids have recently received much attention (Peters et al., 1977; Peacor et al., 1978; Albrecht, 1980; Albrecht and Peters, 1980; Brown et al., 1980; Brown and Huebner, 1981; Gordon et al., 1981). Brown et al. (1980) assembled the then available compositional data and inferred phase equilibria at metamorphic temperatures corresponding to the amphibolite facies for three faces of the $RSiO_3$ tetrahedron (R = Ca–Mg–Fe–Mn). With the recent discovery of the unusually Mn-rich orthopyroxene donpeacorite at Balmat, N. Y. it is now possible to infer the general topology of a phase diagram for the remaining Mn–Mg–Fe face of the $RSiO_3$ tetrahedron. In this paper we describe this mineral and evaluate the pertinent metamorphic phase equilibria.

[1] Contribution No. 389 from the Mineralogical Laboratory of the University of Michigan, Ann Arbor, MI 48109.

[2] Present address: Department of Geology and Geophysics, The University of Utah, Salt Lake City, Utah 84112.

0003–004X/84/0506–0472$02.00

Occurrence and associations

The manganoan orthopyroxene described in this paper occurs in manganese-rich siliceous marbles. Manganese-rich pods are scattered within several of the mappable siliceous marble units at Balmat, N. Y. (Brown et al., 1980). These marbles, which are common throughout the Adirondack Lowlands (Engel and Engel, 1953) were metamorphosed to the upper amphibolite facies (Buddington, 1939) during the 1.0 b.y. old Grenville orogeny. Recent estimates of peak metamorphic conditions at Balmat yield 6.5±1 kbar and 650±30°C (Brown et al., 1978; Bohlen et al., 1980).

Donpeacorite occurs as 1–3 mm interlocking grains making up over 50 percent (modal abundance) of a massive coarse-grained yellow-orange rock. The groundmass consists mainly of the fibrous Mn–Mg amphibole tirodite (40 percent modal abundance), with minor tourmaline, ferrian braunite, manganoan dolomite, hedyphane-like apatite and anhydrite. The tirodite, which is closely associated with the orthopyroxene, is faint orange in hand specimen and colorless in thin-section. The subhedral orthopyroxene is pale buff in hand specimen and faintly pink in thin section. It shows no evidence of twinning or exsolution. Refractive indices were determined in oil on a crystal grain mount (Table 1). The $2V$ was measured on a universal stage using hemispheres with refractive index equal to 1.65 and making no tilt corrections (Table 1).

Chemistry

The pyroxene, amphibole, tourmaline, braunite and hedyphane were analyzed using the University of Michigan ARL-EMX electron microprobe utilizing wavelength dispersive techiques. The operating conditions were 15 kV, 150 μA emission current and 0.015 μA sample current. The standards used were Marjalahti olivine for Si and Mg, Ingamells almandine for Al, synthetic rhodonite for Mn, ANU wollastonite for Ca, Irving kaersutite for Fe and plagioclase (An_{48}) for Na. Corrections for ZAF effects were made using the program EMPADR VII (Rucklidge and Gasparrini, 1969). Two chemical analyses are given in Table 2. The orthopyroxene is rich in manganese, sample 1 having composition $Mg_{1.41}Mn_{0.56}Ca_{0.03}Al_{0.01}Si_{1.98}O_{5.99}$ and sample 2 $Mg_{1.32}Mn_{0.63}Ca_{0.03}Al_{0.01}Si_{2.01}O_{6.01}$ (Fig. 1). The tirodite has significant Ca replacing Mn like those described by Ross et al. (1969). The tourmaline is intermediate between uvite and dravite ($Uv_{46}Dr_{54}$) and is much like the specimen whose structure was refined by Buerger et al. (1962). Semiquantitative analyses of braun-

Table 1. Optical and unit cell parameters of donpeacorite

	Donpeacorite	Enstatite*
	Optical Properties	
α	1.677(2)	1.649
β	1.684(2)	1.653
γ	1.692(2)	1.657
γ−α	0.015	0.008
$2V_x$(meas.)	88(5)	125
	Unit Cell Parameters	
a(Å)	18.384(11)	18.214(4)**
b(Å)	8.879(7)	8.818(2)
c(Å)	5.226(3)	5.177(2)
V(Å^3)	853.12(70)	831.483
D(calc)	3.403(2)	3.21
space group	Pbca	Pbca

*All optical data from Deer, Howie and Zussman (1978),
**All unit cell parameters from Hawthorne and Ito (1977)

Table 2. Electron microprobe analysis of donpeacorite and tirodite

Oxide Weight Percent		Formula	
	Orthopyroxenes[1]		
SiO_2	55.12	Si	1.983
Al_2O_3	0.23	Al	0.010
MnO	18.48	Mn	0.563
MgO	26.31	Mg	1.411
FeO[4]	0.14	Fe	0.004
CaO	0.69	Ca	0.027
Na_2O	0.03	Na	0.003
Total	100.00	O	5.989
		X_{Mn}	0.28
SiO_2	54.64	Si	2.009
Al_2O_3	0.16	Al	0.007
MnO	20.22	Mn	0.630
MgO	24.12	Mg	1.322
FeO[4]	nd	Fe	-
CaO	0.82	Ca	0.032
Na_2O	nd	Na	-
Total	99.96	O	6.013
		X_{Mn}[3]	0.32
	Tirodite[2]		
SiO_2	55.20	Si	7.948
TiO_2	nd	Ti	-
Al_2O_3	1.47	Al^{iv}	0.052
		Al^{vi}	0.197
FeO[4]	0.30	Fe^{2+}	0.036
MgO	22.72	Mg	4.876
MnO	9.47	Mn	1.155
CaO	4.77	Ca	0.736
Na_2O	1.18	Na	0.330
K_2O	nd	K	-
BaO	nd	Ba	-
H_2O[5]	1.26	OH	1.210
F	0.69	F	0.314
Cl	0.01	Cl	0.003
O=F, Cl	-0.29	O	22.479
Total	96.78		

nd, not detected; [1]Normalized to 4 cations;
[2]Normalized as X+Y+Z=15 with all Na in A site;
[3]X_{Mn}=Mn/(Mn+Mg); [4]All Fe assumed as Fe^{2+};
[5]Calculated.

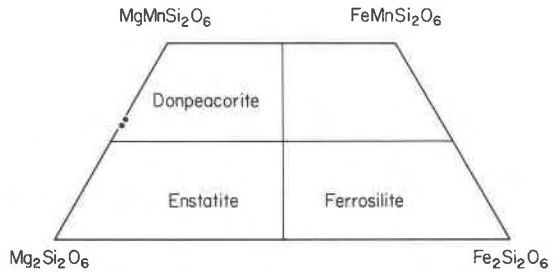

Fig. 1. Orthopyroxene quadrilateral illustrating the donpeacorite compositional field and plot of donpeacorite analyses.

ite and hedyphane show that the braunite is ferrian and the hedyphane is phosphorian.

X-ray crystallography

Donpeacorite and tirodite crystals were studied using single-crystal X-ray techniques. Weissenberg and precission photographs indicated that donpeacorite is orthorhombic. The pattern of extinctions is consistent with space group *Pbca*, the most commonly reported space group for orthopyroxenes (Cameron and Papike, 1980, 1981), and thus it is isostructural with enstatite and hypersthene. Lattice parameters for donpeacorite, refined by least-squares utilizing data from a 1°/min. powder diffractometer pattern internally standardized with quartz, are given in Table 1 and the diffraction data in Table 3. Some of the tirodite displays a faint, light-blue schiller of the kind commonly caused by submicroscopic exsolution lamellae. Exsolution relations have been described in the manganoan amphiboles from the Balmat area by Ross et al. (1969). The presence of submicroscopic exsolution lamellae in our samples was confirmed by Weissenberg photographs which showed a predominant phase having space group *P2/m* intergrown with a much less abundant amphibole, presumably with space group *C2/m*.

Since the standard chemical analysis does not permit an unambiguous structural formula to be calculated, a complete pyroxene structure refinement was undertaken to determine if Mn is ordered into the M2 site. Intensity data were obtained from a cleavage fragment measuring approximately 0.08 × 0.09 × 0.19 mm mounted for rotation about the **c**-axis on a Weissenberg-geometry diffractometer. A Super-Pace automated diffractometer system was used with Mo$K\alpha$ radiation monochromated by a flat graphite crystal and measured with a scintillation counter. A scan was made across each reflection and background were measured on each side. The intensities of 1096 reflections were measured, of which 295 had intensities below the minimum observable values, up to a sine theta limit of 0.461, for h = 0–24, k = 0–12 and l = 0–5. All intensities were corrected for Lorenz-polarization and absorption effects (μ(Mo$k\alpha$) = 28.810 cm^{-1}). A modified version of the program ABSRP written by C. W. Burnham was used for the absorption corrections.

The structure refinement was initiated using parameters for the structure of orthoenstatite given by Hawthorne and Ito (1977). The program RFINE 2 (Finger and Prince, 1975) was employed using the scattering factors of Doyle and Turner (1968), and the weighting scheme of Cruickshank (1965). During the early stages of the refinement the scale factor and atom coordinates were refined, while the occupancies of M1 and M2 were held constant with 100% Mg. In later cycles, refinement of occupancy factors for M1 and M2 was alternated with cycles in which coordinates and/or anisotropic temperature factors were refined. The final unweighted R-value was 5.6 percent for all reflections, and 5.0 percent for all unrejected reflections. Reflections with intensities below the minimum observable value, and those with large individual R-values ($R > 0.5$) were rejected. Final atom positions and temperature factors are listed in Table 4; selected interatomic distances and angles are listed in Table 5; and magnitudes and orientations of the thermal ellipsoids are given in Table 6. The calculated and observed structure factors are listed in Table 7.[3]

Table 3. Principal diffraction lines for donpeacorite

I/Io	d(obs.)	d(calc.)	hkl
10	4.03	4.01,4.05	220, 211*
6	3.24	3.22	411
100	3.18	3.19	420, 221
10	3.09	3.060	600*
10	2.961	2.962	321*
60	2.896	2.896	610*
9	2.847	2.848	511*
9	2.724	2.725	421*
9	2.551	2.551	131*
4	2.531	2.533	611*
10	2.510	2.516	202*
8	2.487, 2.490	2.488, 2.490, 2.493	112, 231, 521
5	2.404	2.406	302
2	2.022	2.025	422
5	2.041	2.040, 2.041	141, 820
5	2.071	2.073, 2.076	512, 721
9	1.9947	-	-
8	1.7420	-	-
11	1.4950	-	-
11	1.4794	-	-
7	1.4019	-	-

CuKa radiation; *Peaks used in refinement.

The final refinement showed an M1 site occupancy of 1.02(1) Mg (and −0.02(1) Mn) and an M2 site occupancy of 0.47(1) Mg and 0.53(1) Mn. Thus the manganese appears to be completely ordered into the M2 site within the sensitivity of the method. Comparison of the suggested composition with that obtained by electron microprobe analysis (first analysis in Table 2) shows that this result is in very good agreement. Analysis 2, which contains slightly more Mn, was obtained on another sample from the same locality. Small amounts of Ca and Fe in the structure are approximately accounted for by the Mn form factor and Al is accounted for by the Mg form factor. The differences from the actual analyses are

[3] To receive a copy of Table 7 order Document AM-84-241 from the business office, Mineralogical Society of America, 200 Florida Avenue, NW, Washington D. C. 20009. Please remit $1.00 in advance for the microfiche.

Table 4. Final atom positions and anisotropic temperature factors ($\times 10^{-5}$)

	X	Y	Z	β_{11}	β_{22}	β_{33}	β_{12}	β_{13}	β_{23}
M1	0.3751(1)	0.6543(2)	0.8721(3)	51(5)	250(20)	550(70)	1(5)	-10(10)	-30(20)
M2	0.3776(1)	0.4801(1)	0.3684(2)	66(3)	340(10)	630(50)	-11(4)	-15(7)	-30(10)
SiA	0.2712(1)	0.3413(1)	0.0484(3)	56(4)	220(10)	520(60)	-7(4)	-16(9)	30(20)
SiB	0.4749(1)	0.3382(1)	0.7949(3)	45(3)	220(10)	600(60)	-10(4)	-13(9)	20(20)
O1A	0.1833(2)	0.3379(3)	0.0407(7)	68(9)	300(40)	610(140)	3(13)	20(20)	-80(40)
O2A	0.3099(2)	0.5022(3)	0.0467(6)	48(8)	280(30)	870(140)	10(10)	10(20)	-10(50)
O3A	0.3017(2)	0.2292(4)	0.8222(7)	72(8)	410(40)	710(140)	4(14)	-40(2)	-30(50)
O1B	0.5632(2)	0.3402(3)	0.7981(7)	58(8)	360(40)	410(140)	5(12)	-20(20)	3(45)
O2B	0.4349(2)	0.4872(4)	0.7028(7)	77(9)	330(40)	1190(150)	20(10)	10(30)	150(50)
O3B	0.4475(2)	0.2050(4)	0.5902(7)	64(8)	430(40)	820(130)	-20(10)	-7(24)	-210(60)

probably somewhat greater than the occupancy factors suggest, but therefore well within the reasonable range of compositional variation in this sample.

Comparison of the detailed structure data obtained for donpeacorite with that for other (Mn,Mg) pyroxenes (Hawthorne and Ito, 1977; Gordon et al., 1981) allows the effects of this ordering to be observed. The ⟨M1–O⟩ bond length of orthoenstatite is 2.076Å, while that for donpeacorite is 2.084Å. If Mn is indeed completely ordered into M2 (and therefore Mg in M1), the ⟨M1–O⟩ distances of donpeacorite and orthoenstatite should be quite similar, as indeed they are. As several authors (Hawthorn and Ito, 1977; Cameron and Papike, 1980) have noted that the ⟨M1–O⟩ bond length is strongly a function of the cation radius, this comparison suggests strongly that Mg is the dominant cation in the M1 site. The slightly larger ⟨M1–O⟩ distance may, however, indicate that some Mn or Fe is present in this site.

Comparison of the ⟨M2–O⟩ distances shows significant differences between donpeacorite and other pyroxenes.

Table 5. Selected interatomic distances and angles

SiA-O1A	1.616(4)	SiB-O1B	1.624(4)
SiA-O2A	1.600(3)	SiB-O2B	1.586(4)
SiA-O3A	1.642(4)	SiB-O3B	1.670(4)
SiA-O3A'	1.659(4)	SiB-O3B'	1.671(4)
⟨SiA-O⟩	1.629	⟨SiB-O⟩	1.638
M1-O1A	2.036(4)	M2-O1A	2.166(3)
M1-O1A'	2.141(4)	M2-O2A	2.104(4)
M1-O2A	2.202(4)	M2-O3A	2.337(4)
M1-O1B	2.068(4)	M2-O3A'	3.542(3)
M1-O1B'	2.187(4)	M2-O1B	2.119(3)
M1-O2B	2.049(4)	M2-O2B	2.044(4)
⟨M1-O⟩	2.114	M2-O3B	2.540(4)
		M2-O3B'	2.994(4)
		⟨M2-O⟩	2.218
O1B-O2B	2.740(5)	O1B-SiB-O2B	117.2(2)
O1B-O3B	2.654(5)	O1B-SiB-O3B	107.3(2)
O1B-O3B'	2.670(5)	O1B-SiB-O3B'	108.2(2)
O2B-O3B	2.657(5)	O2B-SiB-O3B	109.3(2)
O2B-O3B'	2.583(5)	O2B-SiB-O3B'	104.9(2)
O3B-O3B'	2.733(5)	O3B-SiB-O3B'	109.7(1)
⟨O-O⟩	2.673	⟨O-SiB-O⟩	109.4
O1A-O1A	3.041(3)	O1A-M1-O1A	93.4(1)
O1A-O2A	2.978(5)	O1A-M1-O2A	91.3(1)
O1A-O1B	2.828(6)	O1A-M1-O1B	84.8(1)
O1A-O2B	2.806(5)	O1A-M1-O2B	176.9(2)
O1B-O1A	2.839(5)	O1B-M1-O1A	84.4(1)
O1B-O2A	2.841(5)	O1B-M1-O2A	172.9(1)
O1B-1B	3.061(3)	O1B-M1-O1B	92.0(1)
O1B-O2B	3.030(5)	O1B-M1-O2B	95.3(2)
O1A-O2A	3.001(5)	O1A-M1-O2A	95.4(1)
O2A-O2B	2.921(5)	O2A-M1-O2B	91.8(2)
O2B-O1B	3.232(5)	O2B-M1-O1B	94.8(2)
O1B-O1A	2.828(6)	O1B-M101A	81.6(2)
⟨O-O⟩	2.951	⟨O-M1-O⟩	104.6
O1A-O1B	2.828(6)	O1A-M2-O1B	82.6(1)
O1A-O2B	2.806(5)	O1A-M2-O2B	83.5(1)
O1A-O2A	2.952(5)	O1A-M2-O2A	87.5(1)
O1A-O3A	3.670(5)	O1A-M2-O3A	109.1(1)
O1B-O2B	3.035(5)	O1B-M2-O2B	93.6(1)
O1B-O2A	2.841(5)	O1B-M2-O2A	84.5(1)
O1B-O3B	3.032(5)	O1B-M2-O3B'	123.7(1)
O2B-O3A	3.697(5)	O2B-M2-O3A	114.9(1)
O2B-O3B'	2.583(5)	O2B-M2-O3B'	58.1(1)
O2A-O3A	2.525(5)	O2B-M2-O3B	104.4(1)
O2A-O3B	3.084(5)	O2A-M2-O3A	68.8(1)
O2A-O3B	3.138(5)	O2A-M2-O3B'	129.9(1)
O3A-O3B'	3.084(5)	O2A-M2-O3B	84.5(1)
O3A-O3B	2.950(5)	O2A-M2-O3B'	69.4(1)
O3A-O3B'	2.733(3)	O3A-M2-O3B	74.3(1)
⟨O-O⟩	2.997	⟨O-M2-O⟩	91.3
O3A-O3A-O3A	163.8(1)	O3B-O3B-O3B	146.0(3)

Table 6. Magnitude and orientation of the principal axes of the thermal elipsoids

		RMS	Angle to:		
Atom		Displacement	A axis	B axis	C axis
M1	1	0.084(6)	76(20)	71(12)	24(14)
	2	0.093(4)	162(22)	75(24)	81(20)
	3	0.099(4)	79(22)	25(19)	111(13)
M2	1	0.089(3)	72(6)	77(4)	21(6)
	2	0.107(2)	154(7)	104(8)	69(6)
	3	0.117(2)	108(8)	19(7)	96(4)
SiA	1	0.082(4)	79(9)	107(12)	21(8)
	2	0.093(3)	122(14)	146(13)	99(13)
	3	0.102(3)	34(14)	117(14)	108(8)
SiB	1	0.085(3)	32(15)	74(17)	63(24)
	2	0.090(3)	101(27)	129(16)	42(19)
	3	0.099(3)	60(10)	136(16)	118(16)
O1A	1	0.088(10)	103(18)	69(14)	25(17)
	2	0.108(7)	163(39)	84(57)	106(25)
	3	0.113(7)	79(58)	22(20)	109(22)
O2B	1	0.086(8)	21(14)	111(15)	92(15)
	2	0.107(7)	107(22)	146(60)	62(76)
	3	0.111(8)	79(27)	65(70)	28(76)
O3A	1	0.100(8)	51(22)	86(12)	39(21)
	2	0.116(7)	139(23)	72(21)	54(22)
	3	0.129(6)	78(17)	19(21)	104(16)
O1B	1	0.074(12)	72(14)	89(7)	18(14)
	2	0.103(7)	162(15)	85(16)	72(14)
	3	0.120(7)	86(16)	5(16)	92(8)
O2B	1	0.104(7)	113(25)	32(14)	112(13)
	2	0.116(7)	154(23)	105(24)	68(14)
	3	0.141(7)	77(11)	62(9)	31(11)
O3B	1	0.095(8)	68(34)	60(8)	39(22)
	2	0.105(7)	157(33)	83(19)	68(29)
	3	0.140(6)	95(8)	31(7)	120(7)

In order to limit problems due to variable M2 coordination, only average values for the six closest oxygens (O1A, O2A, O3A, O1B, O2B, O3B) will be compared. The ⟨M2–O⟩ distance for orthoenstatite is 2.149Å, that for donpeacorite is 2.218Å, and kanoite and manganoan diopside yield 2.299Å and 2.495Å, respectively. The value for kanoite has been re-averaged from that in Gordon et al. (1981) to account for only the six closest oxygens. As these last two pyroxenes differ structurally from donpeacorite (space groups $P2_1/c$ and $C2c$, respectively), they are not strictly comparable, but should show a similar trend. Comparison of the ⟨M2–O⟩ bond length of orthoenstatite with that for clinoenstatite (2.142Å, space group $P2_1/c$, Ohashi and Finger, 1976) suggests that kanoite is a reasonable analog for a more manganoan donpeacorite in this respect. The occupancy reported for the M2 site in a sample of clinopyroxene with exsolved kanoite by Gordon et al. (1981) is 0.86 Mn, 0.14 Mg. Extrapolating linearly from orthoenstatite and this kanoite to a stoichiometric (1:1) Mn–Mg end-member yields ⟨M2–O⟩ equal to 2.323Å. For the structural effects, we predict a ⟨M2–O⟩ value for donpeacorite of 2.239Å, which is only slightly larger than that actually observed. If the kanoite value is corrected downward approximately 0.01Å to correct for the structural differences, the predicted ⟨M2–O⟩ for donpeacorite is 2.234Å, which is still larger than the measured value. Hawthorne and Ito (1977) show that the relationship between ⟨M2–O⟩ and composition may not be exactly linear, and suggest a correction based on the degree of bond-length distortion Δ:

$$\Delta = \frac{1}{6}\sum_{i=1}^{6}[(R_i - \bar{R})/\bar{R}]^2$$

where $\bar{R}$ is the mean bond length and R_i is the individual bond length. The value calculated for donpeacorite is 5.86×10^{-3} which would give an approximate correction (their Fig. 5) of −0.08Å. Using the above approximation corrected for space group structural effects, we predict a ⟨M2–O⟩ bond length of 2.226Å for donpeacorite, within error of the measured value.

A commonly discussed feature of the pyroxene structure (Papike et al., 1973; Hawthorn and Ito, 1977; Cameron and Papike, 1980, 1981; Gordon et al., 1981) is the O3–O3–O3 angle, which describes the degree of rotation of the tetrahedral chains from the ideal 180° conformation of a straight chain. As the two tetrahedral chains in *Pbca* pyroxenes are not symmetrically related, there are two such angles in donpeacorite, 163.8° for the A-chain and 146.0° for the B-chain. Comparison with other pyroxenes (Cameron and Papike, 1980) shows that the A-chain rotation falls near the average rotation reported, but the B-chain angle is at the extreme upper end of the reported range. The average cation radius in the M1 and M2 sites (Shannon and Prewitt, 1969) is approximately 0.75Å. Comparing this with the plot of average cation ionic radius versus chain angle given by Cameron and Papike (1980, Fig. 28) the A-chain angle agrees well while the B-chain is nearly 2° higher than the trend shown by other orthopyroxenes. The scatter in the data suggests that O3–O3–O3 angles are not a simple function of cation ionic radius.

A similar approach cannot be used to study the relationship between cation ordering and the O3–O3–O3 angles. These angles are quite different in ortho- and clinoenstatite and thus kanoite cannot be used to predict the values for donpeacorite. In addition, as the tetrahedral chains coordinate both octahedral sites, their orientations should reflect an average cation property rather than properties of the individual octahedra.

The (Mg,Fe) orthopyroxenes may be used to model the effect of cation ordering on the O3–O3–O3 angle. Burns (1970) has noted that Fe should order into the M2 site in orthopyroxene due to Jahn–Teller effects. The O3–O3–O3 angle for the A and B chains may be plotted against Fe/(Fe + Mg) or average octahedral cation radius for the series orthoenstatite-orthoferrosilite (Fig. 2). The A-chain angle increases continuously over this range, but the B-chain angle reaches a peak at about 50% Fe, and then levels out and may even decrease towards orthoferrosilite. This suggests that the B-chain angle is more sensitive to the cation in M2 than the cation in M1, and will therefore reflect ordering into the M2 site.

The O3–O3–O3 angles of donpeacorite and a manganoan orthoenstatite synthesized by Hawthorne and Ito (1977) are shown as a function of average octahedral cation radius in Figure 2. While there are insufficient data to be sure whether the (Mn,Mg) orthopyroxenes follow a trend similar to that shown by the (Mg,Fe) orthopyroxenes, the trend suggested by the three available points on this join at least suggests that more than average cation radius affects the O3–O3–O3 angles.

Discussion

Donpeacorite at Balmat occurs in the amphibolite facies, well down-grade from the orthopyroxene isograd

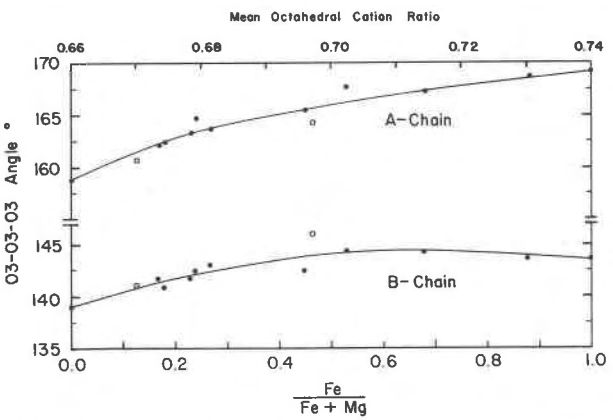

Fig. 2. O3–O3–O3 angle for (Fe,Mg) orthopyroxenes. Sources of data: solid circles—Burnham et al. (1971); Dodd et al. (1975); Ghose (1965); Ghose and Wan (1973); Kosoi et al. (1974); Miyamoto et al. (1975); Smyth (1973); Sueno et al. (1976); Takeda (1972); Takeda and Ridley (1972). Open square—Hawthorne and Ito (1977). Open circle—This paper.

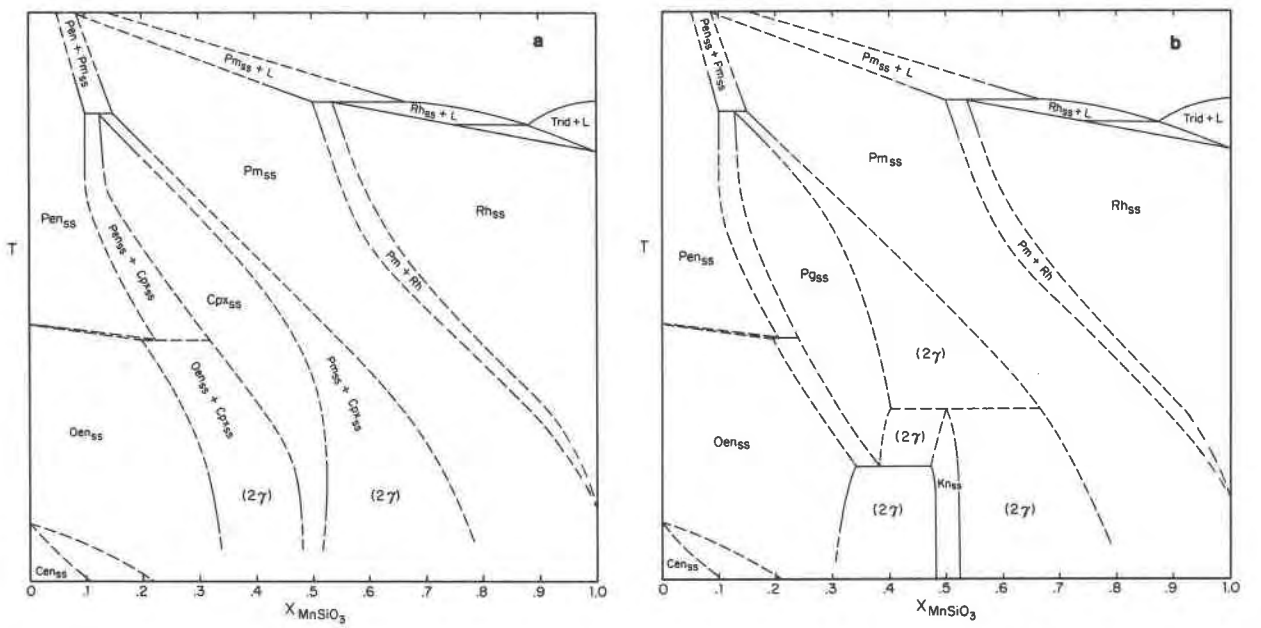

Fig. 3. Two possible configurations of phase equilibria in the system $MnSiO_3$–$MgSiO_3$ consistent with Ito's (1972) high-temperature phase equilibria and with our observations at metamorphic temperatures. Fig. 3a assumes that Ito's manganoan clinopyroxene shows complete solid solution to kanoite. Fig. 3b is drawn assuming that Ito's clinopyroxene disproportionates to orthopyroxene and kanoite similar to pigeonite equilibria in the system $CaSiO_3$–$MgSiO_3$–$FeSiO_3$. The effect of Mn on the orthopyroxene polymorphs is hypothetical but is chosen to avoid interfering with the data of Ito and ours at metamorphic temperatures.

that marks the transition from the amphibolite facies to the granulite facies (Engel and Engel, 1955). The presence of donpeacorite in a marble, however, should not be expected to correspond to the appearance of hypersthene in a metabasite; the substitution of manganese in enstatite or dilution of the fluid phase by CO_2 in the marble may well have locally extended the stability of the orthopyroxene + fluid assemblage at Balmat. Even there the occurrences of manganoan pyroxenes are extremely rare and localities for tirodite (and "hexagonite") are widespread, suggesting that only locally were bulk rock and fluid compositions compatible with the generation of these pyroxenes.

The distribution of Mn/Mg between pyroxene and amphibole is of interest for reactions involving these phases. Ignoring for the present intracrystalline cation distributions, one may calculate the bulk K_D:

$$K_D(\text{bulk}) = \frac{(\text{Mn/Mg})\text{opx}}{(\text{Mn/Mg})\text{amph}} = \frac{0.630/1.320}{1.155/4.876} = 2.015.$$

The partitioning of Mn vs. Mg between orthopyroxene and amphibole may be rationalized in terms of their crystal structures. In the Mn–Mg system, Mn clearly prefers the larger M2 site in pyroxene and the M4 site in amphibole, while Mg is partitioned into M1 in pyroxene and M1, M2, and M3 in amphibole. Thus the approximate upper limit of Mn:Mg expected in pyroxene is 1:1 = M2:M1 and in amphibole it is $2:5 = 2M_4:(2M_1 + 2M_2 + M_3)$. Thus one would predict a K_D of 2.5 for a coexisting $MnMgSi_2O_6$ pyroxene and $Mn_2Mg_5Si_8O_{22}(OH)_2$ tirodite. At Balmat, Ca is also involved in these minerals, and while the manganoan orthopyroxene takes little Ca, the tirodite contains some 37% Ca in M4 (Table 1). Thus Ca displaces Mn in the M4 site of amphiboles while hardly affecting the orthopyroxene and this increases the bulk K_D in Mn:Mg. It therefore appears that the K_D of (Mn/Mg) for pyroxene compared to amphibole is strongly dependent on the availability of calcium for the amphibole.

The distribution coefficient of (Mn/Mg) between the M2 site of pyroxene and the M4 site of amphibole is also instructive. Assuming all Mn in M4 of amphibole and M2 of pyroxene, as shown by the structural refinement,

$$K_D(\text{large site}) = \frac{(\text{Mn/Mg})^{M2}_{Opx}}{(\text{Mn/Mg})^{M4}_{Amph}} = \frac{0.63/0.32}{0.58/0.054} = 0.18$$

This calculation suggests that the M4 site of amphibole prefers Mn over Mg compared to M2 of pyroxene but the significant Ca in the amphibole will probably also affect this K_D (large site).

No experimental data are yet available on the $MgSiO_3$–$MnSiO_3$ binary at metamorphic temperatures, but Ito (1972) has reported on experiments at 1300–1500°C. His experiments show successive fields of orthopyroxene, clinopyroxene, pyroxmangite and rhodonite from $MgSiO_3$ to $MnSiO_3$, but the positions of gaps between these fields

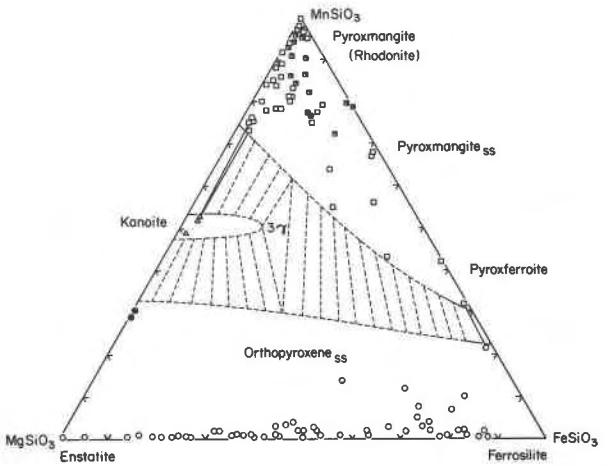

Fig. 4. Compilation of published analyses for the $MnSiO_3$–$FeSiO_3$–$MgSiO_3$ face of the $RSiO_3$ pyroxene–pyroxenoid tetrahedron. P = 4–8 kbar, T = 500–700°C for most of the points. Sources of data: Ford and Bradley (1913); Henry (1935); Tilley (1937); Heitanen (1938); Yosimura (1939); Kuno (1947); Lee (1955); Howie (1964); Momoi (1964); Ewart (1967); Mason (1973); Peters et al. (1973); Marek et al. (1975); Kobayashi (1977); Krogh (1977); Peters et al. (1977); Chopin (1978); Deer et al. (1978); Murthy (1978); Schreyer et al. (1978); Johnson and Knedler (1979); Pavelescu and Pavelescu (1980); Sivaprakash (1980); Fukuoka (1981). The solid circles are the analyses reported in this paper. At the $MnSiO_3$ apex half shaded squares (◪) represent rhodonite analyses in which $X_{CaSiO_3} < 0.07$; open squares (□) represent pyroxmangite analyses. Coexisting minerals are connected by solid lines and those inferred as coexisting are connected by dashed lines.

are considerably different from those inferred from natural assemblages at much lower temperatures (Figs. 3a, 3b). One may speculate that Ito's (1972) clinopyroxene ($En_{87}Rh_{13}$) is a $C2/c$ type continuously changing composition with decreasing temperature to $C2/c$ kanoite ($En_{50}Rh_{50}$) as shown in Figure 3a. Alternatively, Ito's clinopyroxene might be a pigeonite-type structure disproportionating to manganoan enstatite and kanoite at lower temperatures (Fig.3b). Reversed experiments and careful crystallographic observations of synthetic products on the $MgSiO_3$–$MnSiO_3$ binary between 600 and 1100°C are needed to resolve these speculations.

Published data for pyroxenes and pyroxenoids well represented by the subsystem $MnSiO_3$–$MgSiO_3$–$FeSiO_3$ have been plotted in Figure 4. Compositional data and phase identifications were taken directly from the literature. All analyses with $CaSiO_3$ component greater than 7% have been excluded, and only metamorphic pyroxenes and pyroxenoids are plotted. Solid tie-lines connect coexisting minerals while dashed lines connect inferred compositions. From the available data one-, two-, and three-phase regions may be inferred. Orthopyroxene and pyroxmangite solid solutions appear to occupy large one-phase areas of the diagram. Three two-phase fields are present, and a three-phase field orthopyroxene$_{ss}$–pyroxmangite$_{ss}$–kanoite$_{ss}$ must be located somewhere inside the diagram. Only two or three kanoite occurrences are known, and kanoite–donpeacorite pairs have not yet been reported but the manganese-rich pods of the Balmat area may yet yield this assemblage.

The discovery of donpeacorite at Balmat requires some minor revisions of the Brown et al. (1980) phase diagram for the subsystem $MnSiO_3$–$MgSiO_3$–$CaSiO_3$ (their Figs. 2 and 4) with respect to their inferred $MnSiO_3$ solution of orthopyroxene. The field for orthopyroxene along the $MgSiO_3$–$MnSiO_3$ join should be extended towards the clinopyroxene field such that the separation between the two fields is reduced to less than 20 mole %. Unlike the $CaMgSi_2O_6$–$Mg_2Si_2O_6$ system, the $MnMgSi_2O_6$–$Mg_2Si_2O_6$ binary must show extensive solution in the orthopyroxene and Mn must be much more easily accommodated than Ca in the M2 site of the orthopyroxene structure at metamorphic temperatures.

Acknowledgments

We would like to thank the geological staff of St. Joe Minerals Corporation Balmat-Edwards Division for collecting and providing the samples examined in this study. Microprobe funds were provided by the University of Michigan. Thanks are due to the staff of the University of Michigan Microbeam Laboratory for maintenance of the electron microprobe facility. We gratefully acknowledge the help of A. Kato in critically reviewing our submission of donpeacorite as a new mineral to the I.M.A. S. J. Huebner and J. M. Rice are thanked for their thoughtful reviews.

References

Albrecht, J. (1980) Stability relations in the system $CaSiO_3$–$CaMnSi_2O_6$–$CaFeSi_2O_6$. Contributions to Mineralogy and Petrology, 74, 253–260.

Albrecht, J. and Peters, T. (1980) The miscibility gap between rhodonite and bustamite along the join $MnSiO_3$–$Ca_{0.40}Mn_{0.60}SiO_3$. Contributions to Mineralogy and Petrology, 74, 261–269.

Bohlen, S.R., Essene, E.J., and Hoffman, K.S. (1980) Feldspar and oxide thermometry in the Adirondacks: an update. Geological Society of America Bulletin, 91, 110–113.

Brown, P.E., Essene, E.J., and Kelly, W.C. (1978) Sphalerite geobarometry in the Balmat–Edwards district, New York. American Mineralogist, 63, 250–257.

Brown, P.E., Essene, E.J., and Peacor, D.R. (1980) Phase relations inferred from field data for Mn pyroxenes and pyroxenoids. Contributions to Mineralogy and Petrology, 74, 417–425.

Brown, P.E. and Huebner, J.S. (1981) Geothermometry of $(Ca,Fe,Mn)SiO_3$ minerals: the experimental approach. Geological Society of America Abstracts with Program, 13, 418.

Buddington, A.F. (1939) Adirondack Igneous Rocks and their Metamorphism. Geological Society of America Memoir 7.

Buerger, M.J., Burnham, C.W., and Peacor, D.R. (1962) Assessment of the several structures proposed for tourmaline. Acta Crystallographica, 15, 583–590.

Burnham, C.W., Ohashi, Y., Hafner, S.S., and Virgo, D. (1971) Cation distribution and atomic thermal vibrations in an iron-rich orthopyroxene. American Mineralogist, 56, 850–876.

Burns, R.G. (1970) Mineralogical Applications of Crystal Field Theory. Cambridge University Press, London.

Cameron, M. and Papike, J.J. (1981) Structural and chemical variations in pyroxenes. American Mineralogist, 66, 1–50.

Cameron, M. and Papike, J.J. (1980) Crystal chemistry of pyroxenes. In P.S. Ribbe, Ed., Pyroxenes, Vol. 7, p. 5–92. Mineralogical Society of America Reviews in Mineralogy, Washington, D.C.

Chopin, C. (1978) Les Paragenese reduits ou oxides de concentrations manganiferes des "schistes lustres" de Haute- Maurienne (Alpes Francaises). Bulletin de Minéralogie, 101, 514–531.

Cruickshank, D.W.S. (1965) Errors in least-squares methods. In J.S. Rollett, Ed., Computing Methods in Crystallography, p. 112–116. Pergamon Press, Oxford.

Deer, W.A., Howie, R.A., and Zussman, J. (1978) Rock-Forming Minerals, Volume 2A: Single-Chain Silicates. John Wiley and Sons, New York.

Dodd, R.T., Grover, S.E., and Brown, G.E. (1975) Pyroxenes in the Shaw (1–7) chondrite. Geochimica et Cosmochimica Acta, 39, 1585–1594.

Doyle, P.A. and Turner, P.S. (1968) Relativistic Hartree–Fock X-ray and electron scattering factors. Acta Crystallographica, A24, 390–397.

Engel, A.E.J. and Engel, C.G. (1955) Grenville series in the NW Adirondack Mountains, New York: Part 1—General features of the Grenville series, and Part 2—Origin of the major paragneiss. Geological Society of America Bulletin, 64, 1010–1047.

Ewart, A. (1967) Pyroxene and magnetite phenocrysts from the Taupo quaternary rhyolitic pumice deposits, New Zealand. New Zealand Journal of Geology and Geophysics, 180–194.

Finger, L.W. and Prinz, E. (1975) A system of Fortran IV computer programs for crystal structure computations. U.S. National Bureau of Standards, Technical Note 854.

Ford, W.E. and Bradley, W.M. (1913) Pyroxmangite, a new member of the pyroxene group and its alteration product skemmatite. American Journal of Science, 36, 169–174.

Fukuoka, M. (1981) Mineralogical and genetical study of alabandite from the manganese deposits of Japan. Memoirs of the Faculty of Science, Kyushu University, Series D, Geology, 24, 207–251.

Ghose, S. (1965) Mg^{2+}–Fe^{2+} order in an orthopyroxene $Mg_{0.93}Fe_{1.07}Si_2O_6$. Zeitschrift für Kristallographie, 122, 81–99.

Ghose, S. and Wan, C. (1973) Luna 20 pyroxenes: evidence for a complex thermal history. Proceedings of the 4th Lunar Science Conference, 1, 901–907.

Gordon, W.A., Peacor, D.R., Brown, P.E., Essene, E.J., and Allard, L.F. (1981) Exsolution relationships in a clinopyroxene of average composition $Ca_{0.43}Mn_{0.69}Mg_{0.82}Si_2O_6$ from Balmat, New York: X-ray diffraction and scanning transmission electron microscopy. American Mineralogist, 66, 127–144.

Hawthorne, F.C. and Ito, J. (1977) Synthesis and crystal-structure refinement of transition metal orthopyroxenes 1: orthoenstatite and (Mg,Mn,Co) orthopyroxene. Canadian Mineralogist, 15, 321–338.

Heitanen, A. (1938) On the petrology of Finnish quartzites. Bulletin de la Commission Geologique de Finlande, 122, 1–119.

Henry, N.M.F. (1935) Some data on the iron-rich hypersthenes. Mineralogical Magazine, 24, 221–226.

Howie, R.A. (1964) Some orthopyroxenes from the Scottish metamorphic rocks. Mineralogical Magazine, 33, 903–911.

Ito, J. (1972) Rhodonite–pyroxmangite peritectic along the join $MnSiO_3$–$MgSiO_3$ in air. American Mineralogist, 57, 865–876.

Johnson, J.H. and Knedler, K.E. (1979) A Mossbauer spectroscopic study of the cooling history of hypersthenes from selected members of Taupo Pumice Formation, New Zealand. Mineralogical Magazine, 43, 279–285.

Kobayashi, H. (1977) Kanoite $(Mn^{+2},Mg)Si_2O_6$, a new clinopyroxene in the metamorphic rocks from Tatehira, Oshima Peninsula, Hokkaido, Japan. Journal of the Geological Society of Japan, 83, 537–542.

Kosoi, A.L., Malkova, L.A., and Frank-Kamenetskii, V.A. (1974) Crystal-chemical characteristics of orthorhombic pyroxenes. Kristallografiya, 19, 282–288 (transl. Soviet Physics and Crystallography, 19, 171–174).

Krogh, E.J. (1977) Origin and metamorphism of iron formations and associated rocks, Lofoten-Vesteralen, N. Norway 1. The Vestpolltind Fe-Mn deposit. Lithos, 10, 243–255.

Kuno, H. (1947) Hypersthene in a rock of amphibolite facies from Tanzawa Mountainland, Kanagawa perfecture, Japan. Proceedings of the Japan Academy, 23, 113–116.

Lee, D.E. (1955) Mineralogy of Some Japanese Ores. 5, 1–65, Stanford University Press, Palo Alto.

Mason, B. (1973) Manganese silicate minerals from Broken Hill, New South Wales. Journal of the Geological Society of Australia, 20, 397–404.

Miyamoto, M., Takeda, H., and Takano, Y. (1975) Crystallographic studies of a bronzite in the Johnstown achondrite. Fortschritte der Mineralogie, 52, 389–397.

Marek, V., Povondra, P., and Zak, L. (1975) Pyroxmangite, rhodonite and tephroite from Chvaletice, Czechoslovakia. Acta Universitatis Carolinae Geologica, 3, 187–198.

Momoi, H. (1964) Mineralogical study of rhodonites in Japan, with special reference to contact metamorphism. Memoirs of the Faculty of Science, Kyushu University, Series D, Geology, 15, 39–63.

Murthy, D.S.N. (1976) Ortho- and clino-pyroxenes from the granulites of Namakal, Tamil Nadu (Madras), India. Mineralogical Magazine, 40, 788–790.

Ohashi, Y. and Finger, L.W. (1976) The effect of Ca substitution on the structure of clinoenstatite. Carnegie Institution of Washington Year Book, 75, 743–746.

Papike, J.J., Prewitt, C.T., Sueno, S., and Cameron, M. (1973) Pyroxenes: comparisons of real and ideal strutural topologies. Zeitschrift für Kristallographie, 138, 254–273.

Pavelescu, L. and Pavelescu, M. (1980) Chemistry and optical properties of some manganese and iron silicates in the Southern Carpathians. Reviews of Roumanian Geology, Geophysics and Geography, 4, 51–70.

Peacor, D.R., Essene, E.J., Brown, P.E., and Winter, G.A. (1978) The crystal chemistry and petrogenesis of a magnesian rhodonite. American Mineralogist, 63, 1137–1142.

Peters, T., Schwander, H., and Trommsdorf, V. (1973) Assemblages among tephroite, pyroxmangite, rhodochrosite, quartz: Experimental data and occurrences in the Rhetic Alps. Contributions to Mineralogy and Petrology, 42, 325–332.

Peters, T., Valarelli, J.V., Coutinho, J.M.V., Sommeraur, J., and Raumer, J. von (1977) The manganese deposits of Buritirama (Para, Brazil). Schweizerische Mineralogische und Petrographische Mitteilungen, 57, 313–327.

Ross, M., Papike, J.J., and Shaw, K.W. (1969) Exsolution textures in amphiboles as indicators of subsolidus thermal histories. Pyroxenes and Amphiboles: Crystal Chemistry and Phase Petrology. Mineralogical Society of America Special Publication, No.2, 275–299.

Rucklidge, J. and Gasparrini, E.L. (1969) Specifications of a complete program for processing electron microprobe data: EMPADR VII. Department of Geology, University of Toronto, unpublished circular.

Schreyer, W., Stepto, D., Abraham, K., and Muller, W.F. (1978) Clinoeulite (magnesian clinoferrosilite) in a eulysite of a metamorphosed iron formation in the Vredefort structure, South Africa. Contributions to Mineralogy and Petrology, 65, 351–361.

Shannon, R.D. and Prewitt, C.T. (1969) Effective ionic radii in oxides and fluorides. Acta Crystallographica, B25, 925–946.

Sivaprakash, C. (1980) Mineralogy of manganese deposits of Koduru and Garbham, Andhra Pradesh, India. Economic Geology, 75, 1083–1104.

Smyth, J.R. (1973) An orthopyroxene structure up to 850°C. American Mineralogist, 58, 636–648.

Sueno, S., Cameron, M., and Prewitt, C.T. (1976) Orthoferrosilite: high-temperature crystal chemistry. American Mineralogist, 61, 38-53.

Takeda, H. (1972) Crystallographic studies of coexisting aluminan orthopyroxene and augite of high pressure origin. Journal of Geophysical Research, 77, 5798–5811.

Takeda, H. and Ridley, W.I. (1972) Crystallography and chemical trends of orthopyroxene-pigeonite from rock 14310 and coarse fine 12033. Proceedings of the 3rd Lunar Conference, 1, 423–430.

Tilley, C.E. (1973) Pyroxmangite from Inverness-Shire, Scotland. American Mineralogist, 22, 720–727.

Yosimura, T. (1939) Studies on the minerals from the manganese deposit of the Kasa mine, Japan. Journal of the Faculty of Science, Hokkaido Imperial University, Series IV, Geology and Mineralogy, 4:313–452.

Manuscript received, March 9, 1983;
accepted for publication, January 2, 1984.